

## SHORT COMMUNICATION

# High-Copy Transposons from a Pathogen Give Rise to a Conserved sRNA Family with a Novel Host Immunity Target

Lukas Kunz,<sup>1</sup> Manuel Poretti,<sup>1,2</sup> Coraline R. Praz,<sup>1,3</sup> Marion C. Müller,<sup>1,4</sup> Michele Wyler,<sup>1,5</sup> Beat Keller,<sup>1</sup> Thomas Wicker,<sup>1,†</sup> and Salim Bourras<sup>1,6,†</sup>

<sup>1</sup> Department of Plant and Microbial Biology, University of Zürich, Zollikerstrasse 107, CH-8008 Zürich, Switzerland

<sup>2</sup> Department of Biology, University of Fribourg, Chemin du Musée 10, CH-1700 Fribourg, Switzerland

<sup>3</sup> Center of Biotechnology and Genomics of Plants, Polytechnic University of Madrid, Campus de Montegancedo, 28223 Madrid, Spain

<sup>4</sup> Chair of Phytopathology, TUM School of Life Sciences, Technical University of Munich, Emil-Ramann-Str. 2, 85354 Freising-Weihenstephan, Germany

<sup>5</sup> MWSchmid GmbH, Hauptstrasse 34, CH-8750 Glarus, Switzerland

<sup>6</sup> Department of Plant Biology, Swedish University of Agricultural Sciences, Almas Allé 5, 75007 Uppsala, Sweden

Accepted for publication 27 March 2024.

Small RNAs (sRNAs) are involved in gene silencing in multiple ways, including through cross-kingdom transfers from parasites to their hosts. Little is known about the evolutionary mechanisms enabling eukaryotic microbes to evolve functional mimics of host small regulatory RNAs. Here, we describe the identification and functional characterization of *SINE\_sRNAI*, an sRNA family derived from highly abundant short interspersed nuclear element (SINE) retrotransposons in the genome of the wheat powdery mildew pathogen. *SINE\_sRNAI* is encoded by a sequence motif that is conserved in multiple SINE families and corresponds to a functional plant microRNA (miRNA) mimic targeting *Tae\_API*, a wheat gene encoding an aspartic protease only found in monocots. *Tae\_API* has a novel function enhancing both pattern-triggered immunity (PTI) and effector-triggered immunity (ETI), thereby contributing to the cross activation of plant defenses. We conclude that *SINE\_sRNAI* and *Tae\_API* are functional innovations, suggesting the contribution of transposons to the evolutionary arms race between a parasite and its host.

**Keywords:** aspartic protease, *Blumeria*, cross-kingdom RNAi, transposable elements, wheat

Small RNAs (sRNAs) are ancient regulatory elements mediating a variety of RNA interference (RNAi) mechanisms. While several components of the RNAi machinery are conserved across

†Corresponding authors: T. Wicker; [wicker@botinst.uzh.ch](mailto:wicker@botinst.uzh.ch), and S. Bourras; [salim.bourras@slu.se](mailto:salim.bourras@slu.se)

**Funding:** Support was provided by the Schweizerischer Nationalfonds zur Förderung der Wissenschaftlichen Forschung (1003A\_163325, 310030B\_182833, and 310030\_204165), the Universität Zürich Research Priority Program, and the Swedish Research Council for Sustainable Development Early Career Researchers (2020-01007).

**e-Xtra:** Supplementary material is available online.

The author(s) declare no conflict of interest.



Copyright © 2024 The Author(s). This is an open access article distributed under the CC BY-NC-ND 4.0 International license.

eukaryotes, the origin of RNAi competent sRNAs as well as their mode of pairing with a target sequence vary between eukaryote kingdoms (Moran et al. 2017; Shabalina and Koonin 2008). Despite these functional variations, cross-kingdom mobility of sRNAs between fungal pathogens and their plant hosts, resulting in sequence pairing and down-regulation of immunity targets, has been demonstrated (Hua et al. 2018). This illustrates the capacity of eukaryotic microbes to evolve mimics of plant small regulatory RNAs. The most prominent examples are Bc-siR3 and Bc-siR5, two experimentally validated sRNA sequences from the necrotrophic fungus *Botrytis cinerea*, which are capable of cross-kingdom suppression of defense genes in *Arabidopsis thaliana* (Weiberg et al. 2013). Bc-siR3 and Bc-siR5 are not canonical microRNA (miRNA) or short interfering RNA (siRNA) sequences derived from well-defined precursors (Carthew and Sontheimer 2009). Instead, they are encoded within long terminal repeat (LTR) retrotransposons by precursors that do not form a typical miRNA hairpin structure, as is the case for most (805 of 832) *B. cinerea* sRNAs recovered from infected tissue. This is striking because sRNAs derived from transposable elements (TEs) are commonly involved in TE silencing, which is an essential mechanism for the maintenance of genome integrity (Sigman and Slotkin 2016). This raises the question of whether TE-derived sRNAs could also gain new functions in host-pathogen interactions involving obligate biotrophic pathogens, which establish long-lasting parasitic interactions with their host.

*Blumeria graminis* f. sp. *tritici* (*B.g. tritici*, wheat powdery mildew) is an obligate biotrophic fungal plant pathogen that can only survive on living tissues and exhibits strong host specificity, as it can only infect wheat (Troch et al. 2014). Approximately 85% of the *B.g. tritici* genome is derived from TEs with a particularly rich repertoire of non-LTR retrotransposons (Müller et al. 2019) (Supplementary Fig. S1A). Due to its large TE repertoire, its obligate biotrophic lifestyle and its extreme trend toward host specialization (Supplementary Note S1), we hypothesized that *B.g. tritici* represents a potent system to study the evolution of functional plant sRNA mimics from transposable elements. A hallmark of successful mildew infection is the formation of highly specialized feeding structures called haustoria (singular haustorium), which are only found inside a few epidermal cells (Supplementary Note S1) (Hückelhoven and Panstruga 2011). After establishing infection, mildew grows strictly epi-

phytic hyphae, with haustoria being the main interface for molecular exchanges and delivery of virulence factors (such as effector proteins and possibly sRNAs) to its host. Thus, the start of the haustorial stage, which takes place at approximately 2 to 3 days postinoculation, has been consistently shown to be a highly relevant time point for the expression of important virulence factors (bona fide effectors) (Bourras et al. 2018). Furthermore, recent evidence from the closely related powdery mildew of barley (*Blumeria hordei*) supports the hypothesis that haustoria are an interface for cross-kingdom exchange of sRNAs between cereal mildews and their hosts (Kusch et al. 2023).

We sequenced four sRNA libraries derived from three powdery mildew isolates (Bgt\_96224, Bgt\_94202, and Bgt\_JIW2) growing on the susceptible wheat cultivar ‘Chinese Spring’ and one from an uninfected control (Poretti et al. 2020). Samples were collected at 2 days postinoculation which has been previously shown to correspond to the stage of haustorium formation for all three isolates on ‘Chinese Spring’ (Praz et al. 2018). We recovered 2.7 to 3.1 million mildew sRNA reads from infected samples, with each isolate encoding approximately 760,000

unique sequences, suggesting that *B.g. tritici* mobilizes an extremely diverse repertoire of sRNAs during host infection (Supplementary Note S2). All sRNA sequences mapping to the *B.g. tritici* genome ranged between 19 to 23 nucleotides (nt) in size (Fig. 1A) and were largely derived from TEs (64.33%, Fig. 1B; Supplementary Table S1). Long interspersed nuclear elements (LINEs) contributed most sRNA reads, followed by short interspersed nuclear elements (SINEs, Fig. 1C; Supplementary Table S2). SINEs are short, non-autonomous retrotransposons that rely on enzymes encoded by autonomous retrotransposons such as LINEs for their replication. They were of particular interests to us because a previous study in *B.g. tritici* found SINEs to be specifically enriched in the vicinity of effector genes (Müller et al. 2019), which were shown to be highly transcribed during early infection stages of *B.g. tritici* (Praz et al. 2018). Consistent with their frequent association with highly expressed virulence factors, all nine known *B.g. tritici* SINE families produce sRNAs across their entire length during host infection, albeit at varying levels (examples in Fig. 1D; Supplementary Fig. S1B and C), with the *RSX\_Yhi* and *RSX\_Yho* families producing over 11,000

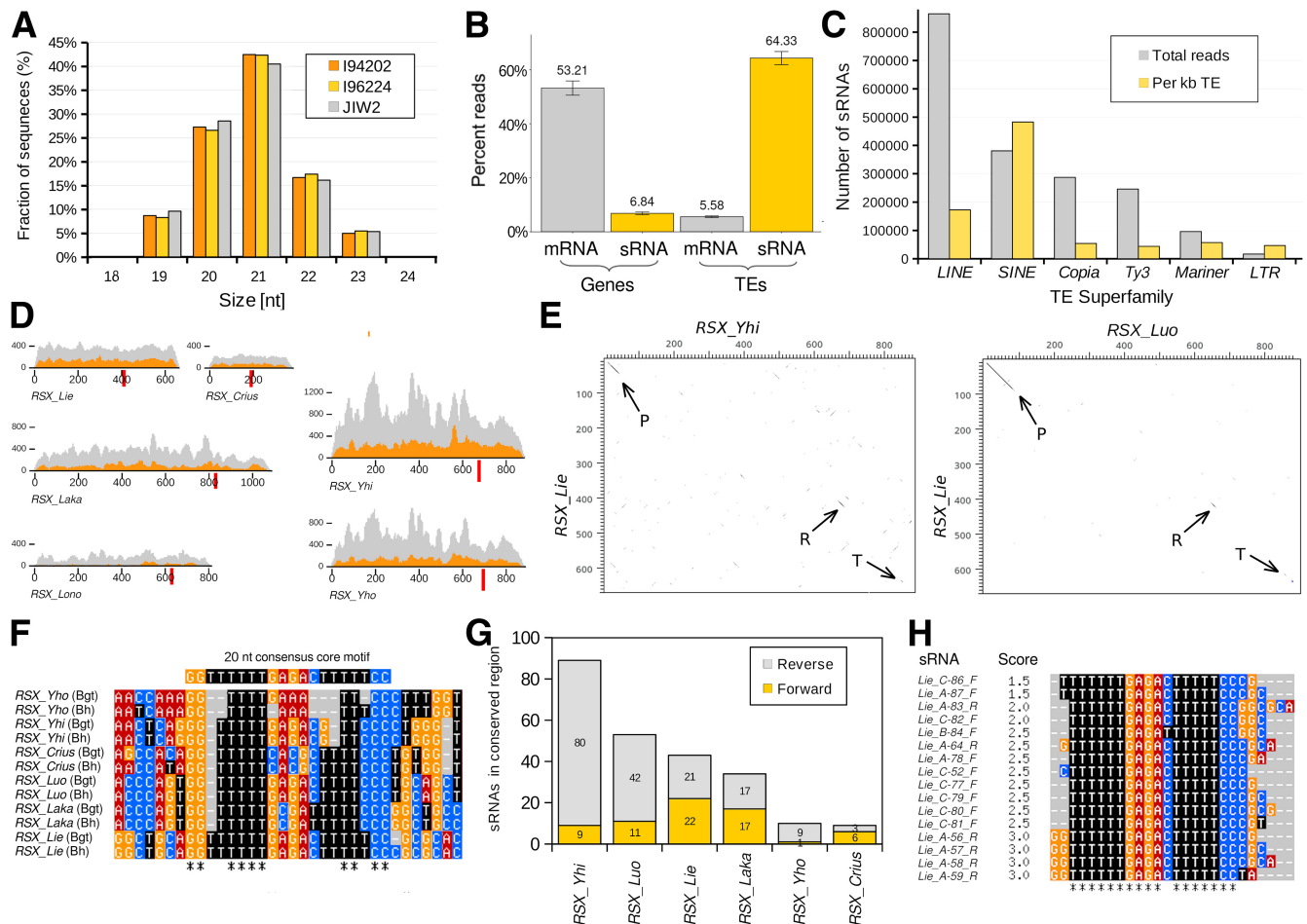


**Fig. 1.** Survey of *Blumeria graminis* f. sp. *tritici* (Bgt) small RNAs (sRNAs) derived from transposable elements. **A**, Size distribution of mildew sRNAs derived from three different isolates. **B**, Transposable elements (TEs) are the largest contributors of sRNAs as compared to genes. An opposite pattern is observed with RNA sequencing reads indicated as mRNA. Asterisks indicate conserved bases. **C**, Fractions of sRNA reads mapped to different mildew TE superfamilies in % of total reads mapping to TEs. *Ty3* indicates the superfamily formally known as “Gypsy”. **D**, Examples showing six short interspersed nuclear element (SINE) families that produce sRNAs over the full TE sequence. The position of the conserved core motif is indicated with a red bar. Sequence coverage with forward sRNA reads is shown in orange, while sequence coverage with reverse reads is stacked on top in gray. **E**, Conserved sequence islands among otherwise highly polymorphic SINEs. P = putative promoter, T = conserved core motif, and R = conserved core motif. **F**, A core 20-nt consensus sequence conserved in SINEs from Bgt and *B. hordei* (Bh) (see also Supplementary Fig. S2A). Asterisks indicate conserved bases. **G**, Number of sRNA variants that contain the core 20-nt conserved motif from individual SINE families. Numbers of forward (sense) and reverse (antisense) variants are shown separately. **H**, Sequence alignment of 16 members of the *SINE\_sRNA1* family derived from *RSX\_Lie* that are predicted to target the wheat gene *TraesCS7D01G475600*. Target prediction was done with the psRNATarget software, and the mapping score is indicated (the lower the better). The sequence at the top was used for subsequent functional validation.

different sequence variants (Supplementary Fig. S1C). Based on these data, we hypothesized that co-expression of SINE-derived sRNAs with fungal effector genes pinpoints their potential role in the establishment of the host-pathogen interaction.

The high number of SINE-derived sRNAs prompted us to further analyze the precursors of such large repertoire across SINEs. Sequence conservation between different SINE families is minimal and usually restricted to short putative promoter and terminator sequences (examples in Fig. 1E). Interestingly, six SINE families contain an additional conserved region in the 3' half, defining a highly conserved 20-nt core sequence motif (Fig. 1D to F; Supplementary Fig. S1B). This core motif is similarly conserved in homologous SINEs in barley powdery mildew (Fig. 1F), indicating that these families diverged before *B.g. tritici* and *B. hordei*, suggesting this region is functionally important alike the putative promoter and terminator sequences (Fig. 1E). This discovery prompted us to focus on the potential evolutionary relevance of this region as precursor of a conserved sRNA family, which here distinguishes our approach from previous studies where highest read abundance has been used as the primary criterion to select for sRNAs of interest. We identified a total of 238 sRNA variants that include this core motif derived from the six SINE families (Supplementary File S1). We hereafter refer to this group of sequences as the *SINE\_sRNA1* family. Here, the *RSX\_Lie* family stood out by exhibiting the highest proportion of sRNA reads mapping in sense orientation (i.e., the transcriptional orientation of the TE, Fig. 1D and G; Supplementary Fig. S1B), indicating these abundant sequences are fulfilling potentially novel functions other than transcriptional silencing of the *RSX\_Lie* family itself. In total, we found 43 *SINE\_sRNA1* variants that are derived from *RSX\_Lie* retrotransposons (examples in Fig. 1H; Supplementary Fig. S2A). Furthermore, the variants containing the 20-nt core motif in *RSX\_Lie* elements showed the lowest sequence diversity of all SINE families, suggesting purifying selection (examples in Fig. 1H; Supplementary Fig. S2).

Given previous reports from *B. cinerea* (Weiberg et al. 2013), recent experimental evidence for cross-kingdom sRNA movement between cereal mildews and their host (Kusch et al. 2023), and transcriptional evidence showing that the *SINE\_sRNA1* family is active during host infection (Müller et al. 2019; Praz et al. 2018), we searched for possible targets of the 43 *SINE\_sRNA1* variants derived from *RSX\_Lie* retrotransposons in the reference hexaploid bread wheat genome, which is derived from the same cultivar infected in this study ('Chinese Spring', IWGSC RefSeq1) (IWGSC et al. 2018). This yielded a list of 35 candidate genes that were targeted by at least 10 different *SINE\_sRNA1* variants (Supplementary Table S3; Supplementary File S2). Manual curation of this gene list in search for a candidate with a potentially novel function in wheat immunity prompted us to focus on *TraesCS7D01G475600* (Supplementary Table S3), which encodes a putative aspartic protease (AP) reminiscent of the barley HORVU6Hr1G071190.3. This homologous AP has been shown to accumulate in the extracellular matrix surrounding haustoria in barley and has been suggested to fulfil an important yet unknown function in the barley immune response to *B. hordei* (Lambertucci et al. 2019). *TraesCS7D01G475600* is predicted to be targeted by several *SINE\_sRNA1* variants through a complementary sequence in the 3' untranslated region (3'UTR) (Supplementary Fig. S3; Supplementary Table S3). Interestingly, sequence analysis of *TraesCS7D01G475600* in the recently published high-quality genome assemblies of 15 diverse wheat cultivars (10+ wheat genomes project, Walkowiak et al. 2020) showed that both the coding sequence and 3'UTR are 100% conserved (Supplementary Note S3; Supplementary Files S3, S4, and S5). Furthermore, we PCR amplified and sequenced the 3'UTR in 94 additional wheat cultivars with diverse breed-

ing histories (WHEALBI project, [Pont et al. 2019]) and found that the full sequence, including the putative *SINE\_sRNA1* binding site, were 100% conserved in all accessions (Supplementary Note S3; Supplementary File S6).

We then sought experimental evidence that *SINE\_sRNA1/TraesCS7D01G475600* is a functional sRNA/target pair. First, using a 21-nt sequence with the highest target prediction score (TTTTTTTGAGACTTTTCCCG, Fig. 1H) as a template for the *SINE\_sRNA1* family, we were able to molecularly isolate, clone, sequence verify, and experimentally validate that *SINE\_sRNA1* can only be found in mildew-infected samples and not in the uninfected control (Fig. 1H; Supplementary Fig. S4; Supplementary Note S4). We assayed the capacity of *SINE\_sRNA1* to exhibit RNAi silencing activity in planta. For this purpose, we designed a silencing-bait assay in the heterologous *Nicotiana benthamiana* system, where a Luciferase (LUC) reporter gene was fused to the 3'UTR of *TraesCS7D01G475600* and transiently co-expressed with an artificial hairpin construct giving rise to *SINE\_sRNA1* (Supplementary Note S5). Consistent with active and specific silencing capacity in planta, the LUC signal was strongly reduced when combined with *SINE\_sRNA1* but remained unaffected by a scrambled version *SINE\_sRNA1\_scr* or when the 3'UTR binding site was mutated (Fig. 2A to E). We conclude that the pathogen-derived *SINE\_sRNA1* family exhibits silencing activity in planta and that the high conservation of its target site in the host suggests that *SINE\_sRNA1* target pairing could take place irrespective of the wheat genotype.

*TraesCS7D01G475600*, hereafter referred to as *Tae\_API*, encodes an AP of the A1 peptidase family. *Tae\_API* carries two catalytic subunits characterized by two indispensable aspartate residues in a conserved DT/SG sequence (Fig. 2F) and localizes to the apoplast upon expression in *N. benthamiana* (Fig. 2G to H). This is consistent with the presence of an N-terminal signal peptide in *Tae\_API* and its high cysteine content, which are often seen for proteins residing in harsh environments like the acidic apoplast (Fig. 2F to I; Supplementary Note S6). Like other A1 peptidases, *Tae\_API* carries a putative inhibitory propeptide (Fig. 2F) whose autocatalytic removal does not occur in a catalytically inactive mutant m*Tae\_API* (D146N, D345N), which was generated by the disruption of both conserved aspartate residues in the catalytic cores (Fig. 2F to I; Supplementary Note S6). Several apoplastic APs have been implicated in plant immunity (Thomas and van der Hoorn 2018; Wang et al. 2020) with prominent, well-characterized examples including *AtCDR1* from *Arabidopsis* and its rice homolog *OsCDR1* (Prasad et al. 2009; Xia et al. 2004). Phylogenetic analysis of AP proteins from *Arabidopsis*, rice, wheat, and eight additional monocots showed that *Tae\_API* is part of a monophyletic clade that is clearly distinct from *CDR1* (Fig. 3A and B; Supplementary Fig. S5; Supplementary Note S7). Comparative sequence analysis including eight additional monocot species revealed *Tae\_API*-like genes to be widespread in monocot species but absent from dicots (Fig. 3B; Supplementary Figs. S5 and S6; Supplementary Note S7; Supplementary File S7), which is striking considering that the *Blumeria* genus can only infect grasses. We further aimed at investigating the molecular contribution of *Tae\_API* to the two canonical layers of plant immune responses triggered against biotrophic parasite like mildews, namely pattern-triggered immunity (PTI) and effector-triggered immunity (ETI) (Jones and Dangl 2006). A hallmark of PTI activation is the production of reactive oxygen species (ROS) upon recognition of conserved pathogen-associated molecular patterns (PAMPs) such as the bacterial flagellin peptide flg22. We therefore tested the impact of *Tae\_API* on ROS production upon flg22-dependent PTI activation using a well-established assay in *N. benthamiana* (Couto and Zipfel 2016). In this ex-

periment, we activated PTI by adding flg22 on the leaf tissue and measured ROS production in the presence of transiently expressed Tae\_AP1, the catalytically inactive mutant mTae\_AP1, or a GUS-negative control. We found that ROS production was strongly increased in the presence of Tae\_AP1 as compared to the catalytically inactive variant mTae\_AP1 (Fig. 3C; Supplementary Note S8) or GUS (Supplementary Fig. S7A), indicating that Tae\_AP1 represents a novel component of plant immunity.

Considering that PTI is a highly conserved immune response against a variety of pathogens, we sought further evidence for a specific role of Tae\_AP1 in wheat defenses against mildew. In this regard, ETI offers an ideal system as such immune responses result from specific recognition of so-called pathogen effector proteins by host intracellular nucleotide-binding leucine-rich-repeat (NLR) receptor proteins (Bourras et al. 2018). These interactions commonly result in a hypersensitive cell-death response (HR, a highly effective response against obligate biotrophs), and several of such effector-NLR pairs have been cloned from the wheat mildew system and functionally validated using transient co-expression assays in *N. benthamiana* (Bourras et al. 2015, 2019; Hewitt et al. 2021; Kunz et al. 2023; Müller et al. 2022; Praz et al. 2017). Furthermore, previous studies have verified that quantitative differences in NLR activation observed in the

*N. benthamiana* system were fully consistent with differences in resistance levels observed in the native wheat host, which has been extensively demonstrated for numerous powdery mildew resistance proteins of the NLR type (including PM2, PM3A, PM3B, PM3C, PM3D, PM3F, and PM17) (Bourras et al. 2019; Lindner et al. 2020; Manser et al. 2021; Müller et al. 2022). We therefore aimed at quantifying the impact of Tae\_AP1 on the strength of the HR resulting from ETI activation by the wheat NLRs PM3 and PM2 using the same assay in *N. benthamiana*. In this experiment, we activated ETI using the previously cloned, functionally validated effector-NLR pairs from *B.g. tritici* and wheat, namely AvrPm3<sup>a2/f2</sup>-Pm3a and AvrPm2-Pm2 (Bourras et al. 2015; Praz et al. 2017), and quantified the strength of the resulting HR in the presence of Tae\_AP1, the catalytically inactive mutant mTae\_AP1, or a GUS-negative control. In both instances, the HR resulting from ETI activation was stronger in the presence of Tae\_AP1 when compared to the inactive variant or GUS (Fig. 3B and C; Supplementary Fig. S7B and C; Supplementary Note S8), indicating that Tae\_AP1 is also implicated in NLR-mediated immune responses of wheat against *B.g. tritici*. NLR proteins can be classified by their N-terminal end consisting of a coiled-coil domain (CC-NLR) (like the wheat PM3A and PM2) or a toll-interleukin domain (TIR-NLR). TIR-

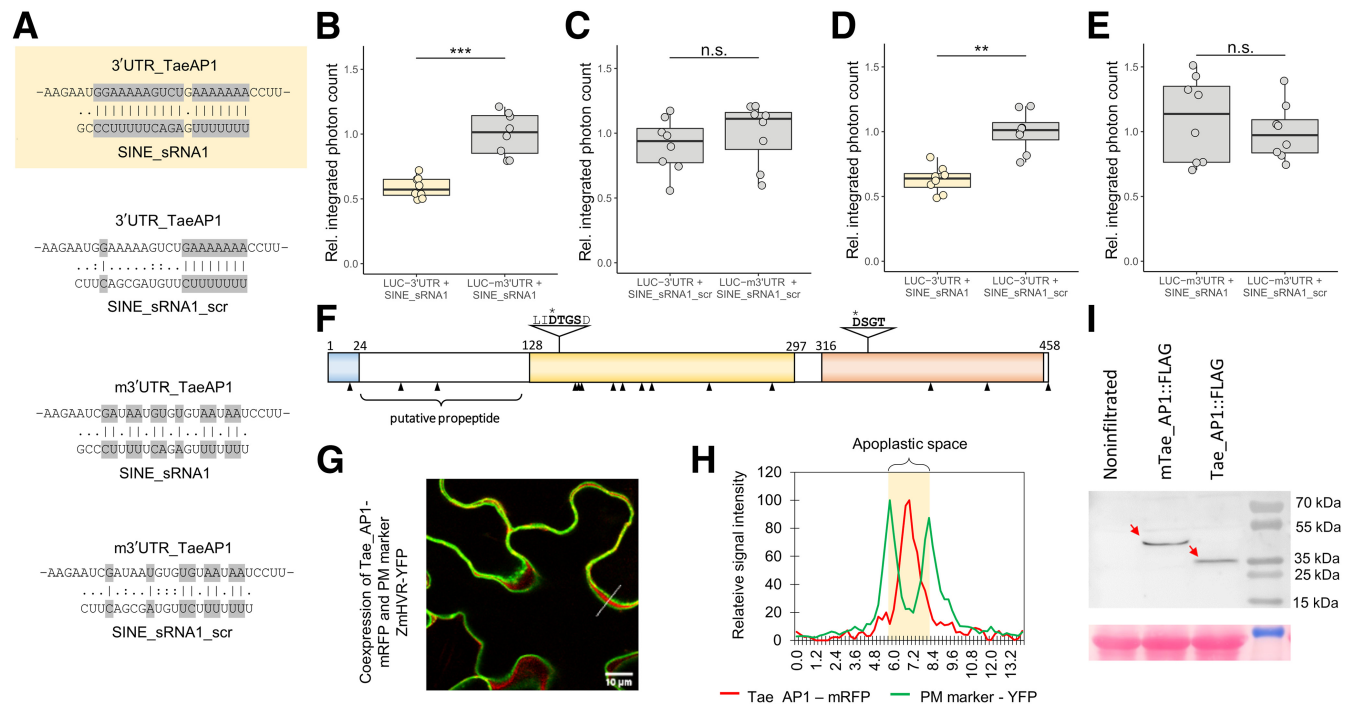


**Fig. 2.** *SINE\_sRNA1* is a functional plant small RNA (sRNA) mimic with silencing activity towards the wheat apoplastic aspartic protease Tae\_AP1 (TraesCS7D01G475600). **A to E**, Luciferase (LUC) reporter-based silencing-bait assay confirming specific silencing activity of *SINE\_sRNA1* towards the 3' untranslated region (3'UTR) of *Tae\_AP1*. **A**, Sequence alignment between the sRNA target site in the 3'UTR of *Tae\_AP1* or a mutated version of the target site (m3'UTR\_TaeAP1) and *SINE\_sRNA1* or a scrambled version *SINE\_sRNA1\_scr*. All tested combinations are depicted. Complementary bases are indicated by vertical bars and highlighted in grey. Wobble positions (U:G) are indicated by colons. Noncomplementary bases are marked by a dot. The combination with predicted silencing capacity in silico is highlighted by a yellow box. **B to E**, LUC activity measured in *Nicotiana benthamiana* leaves co-expressing the LUC-3'UTR reporter and *SINE\_sRNA1* (yellow) or mutated/scrambled versions thereof (grey). All possible pairwise combinations were tested on separate leaves ( $n = 8$ ), verifying that efficient silencing of the LUC reporter only occurs in the presence of the intact sRNA target site and the original *SINE\_sRNA1* sequence. The statistical significance and associated  $P$  value are indicated for each pairwise comparison (Wilcoxon signed-rank test). Stars indicate statistical significance as follows: \*  $P < 0.05$ , \*\*  $P < 0.01$ , and \*\*\*  $P < 0.001$ . n.s. indicates not significant. Assays were replicated three times with identical results. **F**, Schematic depiction of the predicted domain structure of Tae\_AP1. The predicted signal peptide (blue) and the two active domains (yellow TAXI\_N [PF14543]; red TAXI\_C [PF14541]) are highlighted, and flanking residues are numbered. Sequences at the two active sites are magnified with the indispensable aspartate residues (D146, D345) marked by a star. Position of cysteine residues are marked by a triangle, and the extent of the putative propeptide is highlighted. **G**, Tae\_AP1-mRFP (red) apoplastic localization in *N. benthamiana* in comparison to a ZmHVR-YFP plasma membrane marker (green) revealed by confocal microscopy. **H**, Plasmamembrane cross-section quantification of fluorescence signal along the axis (white line) indicated in **G**. **I**, Western blot analysis of Tae\_AP1 and mTae\_AP1 C-terminally fused to a FLAG epitope tag and transiently expressed in *N. benthamiana*. Protein extracts from noninfiltrated leaf areas are shown for comparison. The observed size shift corresponding to the autocatalytic removal of the propeptide (approximately 10 kDa) is indicated by red arrows. A total protein loading control, stained by Ponceau S, is provided in the bottom panel.

NLRs also activate ETI and induce HR upon effector recognition, but this class of receptors is not found in monocots (Tamborski and Krasileva 2020; Tarr and Alexander 2009). Considering the finding that *Tae\_AP1* belongs to a monocot-specific clade, we tested the contribution of *Tae\_AP1* to the ETI mediated by the TIR-NLRs *Rps4/Rrs1* from *Arabidopsis* and *Roq1* from *N. benthamiana* upon recognition of the *Pseudomonas syringae* pv. *tomato* effectors *AvrRps4* and *HopQ1*, respectively (Gassmann et al. 1999; Schultink et al. 2017). Using the same HR quantification assay in *N. benthamiana*, we found that *Tae\_AP1* had no visible effect on the ETI response triggered by TIR-NLRs from dicots (Fig. 3D and E; Supplementary Fig. S7D and E), further substantiating the phylogenetic evidence indicating this gene is a genuine innovation of monocots. We conclude that *Tae\_AP1* fulfills a novel function in the activation of both layers of plant immunity, thereby supporting recent breakthrough findings indicating that ETI execution involves a re-potentialization of PTI (Lu and Tsuda 2021; Yuan et al. 2021) (Supplementary Note S8).

In summary, we propose that small “islands” of sequence conservation across large arrays of otherwise sequence-divergent transposons may provide a springboard for the evolution of conserved sRNA families (like the *SINE\_sRNA1*) from precursors that do not form a typical hairpin. We speculate that such mechanisms are probably common in fungi considering that conserved sRNAs in *B. cinerea* are also derived from transposons. We also propose that the *SINE\_sRNA1* target *Tae\_AP1* encodes a potentially novel function in plant immunity in monocots, suggesting there is larger variety of lineage-specific mechanisms underlying the execution of ETI and PTI responses. Considering the novelty of the *SINE\_sRNA1/Tae\_AP1* pair, we argue that our approach to explore sRNA biology in fungal pathogens, with a primary focus on the origin and evolution of sRNA families, is a potent complement to classical approaches focusing solely on most highly abundant sRNA families. Finally, we propose that both *SINE\_sRNA1* and *Tae\_AP1* are recent innovations driven by the ongoing co-evolutionary arms-race between grass powdery mildews and their hosts. However, our study only characterized

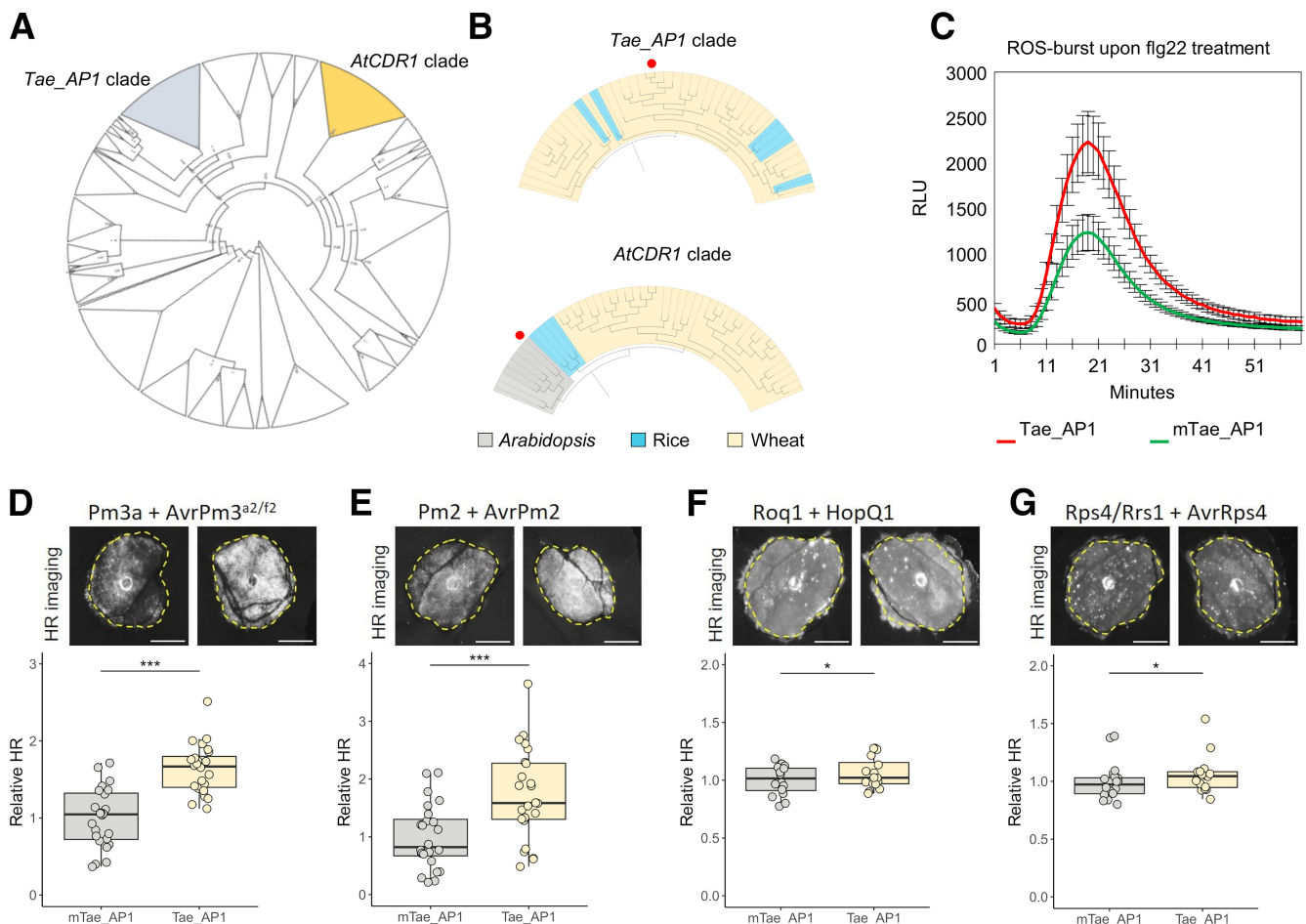


**Fig. 3.** *Tae\_AP1* belongs to a monocot-specific branch of aspartic proteases and is a potent enhancer of pattern-triggered immunity (PTI) and effector-triggered immunity (ETI) immune responses. **A and B**, Phylogenetic analysis of aspartic proteases from *Arabidopsis*, rice, and wheat. **A**, *Tae\_AP1* and *AtCDR1*-like genes belong to distinct clades. **B**, Magnification of the *Tae\_AP1* and *AtCDR1* clades depicted in **A**. The *Tae\_AP1* clade is unique to monocot species. Positions of *Tae\_AP1* and *AtCDR1* are highlighted by a red dot. A full-resolution figure of the phylogenetic analysis depicted in **A** and **B** can be found as Supplementary Figure S5. **C**, Reactive oxygen species (ROS) production upon the bacterial flagellin peptide flg22 challenge of *Nicotiana benthamiana* leaves transiently expressing *Tae\_AP1* (red) or the proteolytically inactive mutant *mTae\_AP1* (green) over 60 min. Results are presented as mean  $\pm$  standard error of the mean. Assays were replicated three times with similar results. **D and E**, *Tae\_AP1* enhances coiled-coiled domain nucleotide-binding leucine-rich-repeat (CC-NLR)-mediated cell death when transiently co-expressed in *N. benthamiana* with *Pm3a* (**D**) and *Pm2* (**E**) and their cognate avirulence effectors *AvrPm3<sup>a2/f2</sup>* and *AvrPm2*, respectively. **F and G**, *Tae\_AP1* marginally affects toll-interleukin domain nucleotide-binding leucine-rich-repeat (TIR-NLR)-mediated cell death with no visible difference observed when transiently co-expressed with *Roq1* (**F**) or *Rps4/Rrs1* (**G**) and their cognate avirulence effectors *HopQ1* and *AvrRps4*, respectively. Scale bars in hypersensitive cell-death response (HR) images correspond to 1 cm. Statistical significance and associated *P* values are indicated for each pairwise comparison (Wilcoxon signed-rank test). Assays were replicated three times with identical results. Stars indicate statistical significance as follows: \* *P* < 0.05, \*\* *P* < 0.01, and \*\*\* *P* < 0.001.

a small subset of large and sequence-diverse sRNA families with potentially thousands of precursors spread across the genome. To better understand the complexity of interactions of sRNAs with their targets, future research will require large scale parallel sequencing of mRNAs, sRNA, and degradomes from both hosts and pathogens at multiple time points during the disease cycle.

## Materials and Methods

A detailed description of all material and methods used in this study is available in the Supplementary Methods online. Sample generation, RNA extraction, and sequencing are described in Supplementary Methods Section 1. The sRNA data processing, bioinformatic analyses, and sRNA target prediction are described in Supplementary Methods Section 2. Phylogenetic analyses and assessment of sequence diversity in *Triticeae* are described in Supplementary Methods Section 3. Stem-loop PCR-based validation of the *SINE\_sRNA1* family is described in Supplementary Methods Section 4. All cloning procedures are described in Supplementary Methods Section 5. Transient gene expression in *N. benthamiana* including all downstream analyses (silencing bait assay, ROS burst measurements, hypersensitive response quantification, and confocal microscopy) are described in Supplementary Methods Section 6. Protein extraction and western blotting are described in Supplementary Methods Section 7. The sRNA sequencing reads are available under the National Center for Biotechnology Information (NCBI) BioProject PRJNA553193 and PRJNA577532 (Poretti et al. 2020).

## Acknowledgments

We thank Prof. Dr. Jonathan D. G. Jones for kindly providing *Rrs1-R*, *Rps4*, and *AvrRps4* genes in the binary vector pICH86988 and Prof. Dr. Frank L. W. Takken for sharing the pBin19-ZmHVR-YFP plasmid. We would also like to express our gratitude to Prof. Dr. Detlef Weigel for sharing the pNW55 plasmid. Furthermore, we thank Dr. Julien Gronnier for critical advice on confocal microscopy and would like to acknowledge the technical support from Gerhard Herren, Helen Zbinden, and Karl Huwiler from the University of Zurich and Dr. Sirisha Aluri from the Functional Genomics Center Zurich (FGCZ).

## Literature Cited

Bourras, S., Kunz, L., Xue, M. F., Praz, C. R., Müller, M. C., Kälin, C., Schläfli, M., Ackermann, P., Flückiger, S., Parlange, F., Menardo, F., Schaefer, L. K., Ben-David, R., Roffler, S., Oberhaensli, S., Widrig, V., Lindner, S., Isaksson, J., Wicker, T., Yu, D. Z., and Keller, B. 2019. The *AvrPm3-Pm3* effector-NLR interactions control both race-specific resistance and host-specificity of cereal mildews on wheat. *Nat. Commun.* 10:2292.

Bourras, S., McNally, K. E., Ben-David, R., Parlange, F., Roffler, S., Praz, C. R., Oberhaensli, S., Menardo, F., Stirnweis, D., Frenkel, Z., Schaefer, L. K., Flückiger, S., Treier, G., Herren, G., Korol, A. B., Wicker, T., and Keller, B. 2015. Multiple avirulence loci and allele-specific effector recognition control the *Pm3* race-specific resistance of wheat to powdery mildew. *Plant Cell* 27:2991-3012.

Bourras, S., Praz, C. R., Spanu, P. D., and Keller, B. 2018. Cereal powdery mildew effectors: A complex toolbox for an obligate pathogen. *Curr. Opin. Microbiol.* 46:26-33.

Carthew, R. W., and Sontheimer, E. J. 2009. Origins and mechanisms of miRNAs and siRNAs. *Cell* 136:642-655.

Couto, D., and Zipfel, C. 2016. Regulation of pattern recognition receptor signalling in plants. *Nat. Rev. Immunol.* 16:537-552.

Gassmann, W., Hirsch, M. E., and Staskawicz, B. J. 1999. The Arabidopsis RPS4 bacterial-resistance gene is a member of the TIR-NBS-LRR family of disease-resistance genes. *Plant J.* 20:265-277.

Hewitt, T., Müller, M. C., Molnár, I., Mascher, M., Holušová, K., Šimková, H., Kunz, L., Zhang, J., Li, J., Bhatt, D., Sharma, R., Schudel, S., Yu, G., Steuernagel, B., Periyannan, S., Wulff, B., Ayliffe, M., McIntosh, R., Keller, B., Lagudah, E., and Zhang, P. 2021. A highly differentiated region of wheat chromosome 7AL encodes a *Pm1a* immune receptor that recognises its corresponding *AvrPm1a* effector from *Blumeria graminis*. *New Phytol.* 229:2812-2826.

Hua, C., Zhao, J.-H., and Guo, H.-S. 2018. Trans-kingdom RNA silencing in plant-fungal pathogen interactions. *Mol. Plant* 11:235-244.

Hückelhoven, R., and Panstruga, R. 2011. Cell biology of the plant-powdery mildew interaction. *Curr. Opin. Plant Biol.* 14:738-746.

International Wheat Genome Sequencing Consortium (IWGSC), Appels, R., Eversole, K., Stein, N., Feuillet, C., Keller, B., Rogers, J., Pozniak, C. J., Choulet, F., Distelfeld, A., Poland, J., Ronen, G., Sharpe, A. G., Barad, O., Baruch, K., Keeble-Gagnère, G., Mascher, M., Ben-Zvi, G., Josselin, A.-A., Himmelbach, A., Balfourier, F., Gutierrez-Gonzalez, J., Hayden, M., Koh, C., Muehlbauer, G., Pasam, R. K., Paux, E., Rigault, P., Tibbits, J., Tiwari, V., Spannagl, M., Lang, D., Gundlach, H., Haberer, G., Mayer, K. F. X., Ormanbekova, D., Prade, V., Šimková, H., Wicker, T., Swarbreck, D., et al. 2018. Shifting the limits in wheat research and breeding using a fully annotated reference genome. *Science* 361:eaar7191.

Jones, J. D. G., and Dangl, J. L. 2006. The plant immune system. *Nature* 444:323-329.

Kunz, L., Sotiropoulos, A. G., Graf, J., Razavi, M., Keller, B., and Müller, M. C. 2023. The broad use of the *Pm8* resistance gene in wheat resulted in hypermutation of the *AvrPm8* gene in the powdery mildew pathogen. *BMC Biol.* 21:29.

Kusch, S., Singh, M., Thieron, H., Spanu, P. D., and Panstruga, R. 2023. Site-specific analysis reveals candidate cross-kingdom small RNAs, tRNA and rRNA fragments, and signs of fungal RNA phasing in the barley-powdery mildew interaction. *Mol. Plant Pathol.* 24:570-587.

Lambertucci, S., Orman, K. M., Das Gupta, S., Fisher, J. P., Gazal, S., Williamson, R. J., Cramer, R., and Bindschedler, L. V. 2019. Analysis of barley leaf epidermis and extrahaustorial proteomes during powdery mildew infection reveals that the PR5 thaumatin-like protein TLP5 is required for susceptibility towards *Blumeria graminis* f. sp. *hordei*. *Front. Plant Sci.* 10:1138.

Lindner, S., Keller, B., Singh, S. P., Hasenkamp, Z., Jung, E., Müller, M. C., Bourras, S., and Keller, B. 2020. Single residues in the LRR domain of the wheat PM3A immune receptor can control the strength and the spectrum of the immune response. *Plant J.* 104:200-214.

Lu, Y., and Tsuda, K. 2021. Intimate association of PRR- and NLR-mediated signaling in plant immunity. *Mol. Plant-Microbe Interact.* 34:3-14.

Manser, B., Koller, T., Praz, C. R., Roulin, A. C., Zbinden, H., Arora, S., Steuernagel, B., Wulff, B. B. H., Keller, B., and Sánchez-Martín, J. 2021. Identification of specificity-defining amino acids of the wheat immune receptor *Pm2* and powdery mildew effector *AvrPm2*. *Plant J.* 106:993-1007.

Moran, Y., Agron, M., Praher, D., and Technau, U. 2017. The evolutionary origin of plant and animal microRNAs. *Nat. Ecol. Evol.* 1:0027.

Müller, M. C., Kunz, L., Schudel, S., Lawson, A. W., Kammerecker, S., Isaksson, J., Wyler, M., Graf, J., Sotiropoulos, A. G., Praz, C. R., Manser, B., Wicker, T., Bourras, S., and Keller, B. 2022. Ancient variation of the *AvrPm17* gene in powdery mildew limits the effectiveness of the introgressed rye *Pm17* resistance gene in wheat. *Proc. Natl. Acad. Sci. U.S.A.* 119:e2108808119.

Müller, M. C., Praz, C. R., Sotiropoulos, A. G., Menardo, F., Kunz, L., Schudel, S., Oberhänsli, S., Poretti, M., Wehrli, A., Bourras, S., Keller, B., and Wicker, T. 2019. A chromosome-scale genome assembly reveals a highly dynamic effector repertoire of wheat powdery mildew. *New Phytol.* 221:2176-2189.

Pont, C., Leroy, T., Seidel, M., Tondelli, A., Duchemin, W., Armisen, D., Lang, D., Bustos-Korts, D., Goué, N., Balfourier, F., Molnár-Láng, M., Lage, J., Kilian, B., Özkan, H., Waite, D., Dyer, S., Letellier, T., Alaux, M., Wheat and Barley Legacy for Breeding Improvement (WHEALBI) consortium, Russell, J., Keller, B., van Eeuwijk, F., Spannagl, M., Mayer, K. F. X., Waugh, R., Stein, N., Cattivelli, L., Haberer, G., Charmet, G., and Salse, J. 2019. Tracing the ancestry of modern bread wheats. *Nat. Genet.* 51:905-911.

Poretti, M., Praz, C. R., Meile, L., Kälin, C., Schaefer, L. K., Schläfli, M., Widrig, V., Sanchez-Vallet, A., Wicker, T., and Bourras, S. 2020. Domestication of high-copy transposons underlies the wheat small RNA response to an obligate pathogen. *Mol. Biol. Evol.* 37:839-848.

Prasad, B. D., Creissen, G., Lamb, C., and Chattoo, B. B. 2009. Overexpression of rice (*Oryza sativa* L.) *OsCDRI* leads to constitutive activation of defense responses in rice and *Arabidopsis*. *Mol. Plant-Microbe Interact.* 22:1635-1644.

Praz, C. R., Bourras, S., Zeng, F. S., Sánchez-Martín, J., Menardo, F., Xue, M. F., Yang, L. J., Roffler, S., Böni, R., Herren, G., McNally, K. E., Ben-David, R., Parlange, F., Oberhaensli, S., Flückiger, S., Schäfer, L. K., Wicker, T., Yu, D. Z., and Keller, B. 2017. *AvrPm2* encodes an RNase-like avirulence effector which is conserved in the two different specialized forms of wheat and rye powdery mildew fungus. *New Phytol.* 213:1301-1314.

- Praz, C. R., Menardo, F., Robinson, M. D., Müller, M. C., Wicker, T., Bourras, S., and Keller, B. 2018. Non-parent of origin expression of numerous effector genes indicates a role of gene regulation in host adaptation of the hybrid triticale powdery mildew pathogen. *Front. Plant Sci.* 9:49.
- Schultink, A., Qi, T., Lee, A., Steinbrenner, A. D., and Staskawicz, B. 2017. Roq1 mediates recognition of the *Xanthomonas* and *Pseudomonas* effector proteins XopQ and HopQ1. *Plant J.* 92:787-795.
- Shabalina, S. A., and Koonin, E. V. 2008. Origins and evolution of eukaryotic RNA interference. *Trends Ecol. Evol.* 23:578-587.
- Sigman, M. J., and Slotkin, R. K. 2016. The first rule of plant transposable element silencing: Location, location, location. *Plant Cell* 28:304-313.
- Tamborski, J., and Krasileva, K. V. 2020. Evolution of plant NLRs: From natural history to precise modifications. *Annu. Rev. Plant Biol.* 71: 355-378.
- Tarr, D. E. K., and Alexander, H. M. 2009. TIR-NBS-LRR genes are rare in monocots: Evidence from diverse monocot orders. *BMC Res. Notes* 2:197.
- Thomas, E. L., and van der Hoorn, R. A. L. 2018. Ten prominent host proteases in plant-pathogen interactions. *Int. J. Mol. Sci.* 19:639.
- Troch, V., Audenaert, K., Wyand, R. A., Haesaert, G., Höfte, M., and Brown, J. K. M. 2014. *Formae speciales* of cereal powdery mildew: Close or distant relatives? *Mol. Plant Pathol.* 15:304-314.
- Walkowiak, S., Gao, L., Monat, C., Haberer, G., Kassa, M. T., Brinton, J., Ramirez-Gonzalez, R. H., Kolodziej, M. C., Delorean, E., Thambugala, D., Klymiuk, V., Byrns, B., Gundlach, H., Bandi, V., Siri, J. N., Nilsen, K., Aquino, C., Himmelbach, A., Copetti, D., Ban, T., Venturini, L., Bevan, M., Clavijo, B., Koo, D.-H., Ens, J., Wiebe, K., N'Diaye, A., Fritz, A. K., Gutwin, C., Fiebig, A., Fosker, C., Fu, B. X., Accinelli, G. G., Gardner, K. A., Fradgley, N., Gutierrez-Gonzalez, J., Halstead-Nussloch, G., Hatakeyama, M., Koh, C. S., Deek, J., et al. 2020. Multiple wheat genomes reveal global variation in modern breeding. *Nature* 588: 277-283.
- Wang, Y., Wang, Y., and Wang, Y. 2020. Apoplastic proteases: Powerful weapons against pathogen infection in plants. *Plant Commun.* 1:100085.
- Weiberg, A., Wang, M., Lin, F.-M., Zhao, H., Zhang, Z., Kaloshian, I., Huang, H.-D., and Jin, H. 2013. Fungal small RNAs suppress plant immunity by hijacking host RNA interference pathways. *Science* 342: 118-123.
- Xia, Y. J., Suzuki, H., Borevitz, J., Blount, J., Guo, Z. J., Patel, K., Dixon, R. A., and Lamb, C. 2004. An extracellular aspartic protease functions in *Arabidopsis* disease resistance signaling. *EMBO J.* 23:980-988.
- Yuan, M., Ngou, B. P. M., Ding, P., and Xing, X.-F. 2021. PTI-ETI crosstalk: An integrative view of plant immunity. *Curr. Opin. Plant Biol.* 62: 102030.